

## ELECTRON DIFFRACTION STUDY OF CuGaS<sub>2</sub>FILM

### Abstract

In present work, the results of electron diffraction investigations of structures of amorphous thin films of CuGaS<sub>2</sub> have been given and function of radial distribution of atoms (FRDA) has been calculated. Appropriate coordination number  $n=4,1$  we obtained from calculating the area under the first peak, also indicates tetrahedral surrounded by atoms of copper and gallium. During the deposition of this ternary compound on a substrate with  $T = 423-433$  K the mixture of polycrystalline single crystal is formed. With the increase of temperature the intensity of polycrystallines decreases and point reflections according to the monocrystal increases. Further increase of the substrate temperature to 453 K LiF leads to the formation of a perfect single crystal.

Superstructure phase CuGaS<sub>2</sub> is oriented on (100) plane parallel to the faces LiF. During epitaxial growth on LiF CuGaS<sub>2</sub> one unit cell superstructure is mated with four cells of the substrate. Between periods of lattices of the initial phase and superstructure there are simple relations common with:  $a \approx 3a_0$ ;  $c \approx 2c_0$ .

**Keywords.** Diffraction, phase, atoms, structure, superstructure, amorphous, compositions

### 1. Introduction.

A number of works [1-3] were devoted to X-ray studies of crystalline structures of the compounds of group A<sup>1</sup>-B<sup>3</sup>-C<sup>6</sup>. However in none of the known works

27 patterns of short range order structure of amorphous compositions  $\text{CuGaS}_2$  were  
28 determined.

29 The reason for this can be found either by difficulties in establishing  
30 conditions for amorphous films of these compounds, or trends in amorphous films to the  
31 more dense packing.

32 Amorphous thin films  $\text{CuGaS}_2$   
33 of thickness 25 nm were obtained by evaporational alloys  $\text{CuGaS}_2$  in the vacuum of  $10^{-4}$   
34 PA on the substrate  $\text{NaCl}$ ,  $\text{KCl}$  and  $\text{LiF}$  located at room temperature.  $\text{NaCl}$ ,  $\text{KCl}$  and  $\text{LiF}$   
35 ion crystals have been chosen as substrate because by solving these crystals in  
36 the water thin  $\text{CuGaS}_2$  layers formed on them separating stay on the surface of water  
37 and which is kept in the metal net with diameter of 0.1-0.3 mm.

38 On the other hand these substrates with cubic structure of different elementary cell  
39 parameters affect epitoxially on crystallisation in primary formation of condensate and  
40 further thermo-  
41 processing. The rate of deposition of films for all cases was the 1.5 nm/sec. Amorphous p  
42 hase  $\text{CuGaS}_2$  is formed until  $T_s=383$  K, crystallization,  
43 which can lead to the formation of polycrystalline with periods of a tetragonal lattice,  
44 military data [5].

45 Amorphous films formed with values  $S=4\pi\sin\theta/\lambda=24.10; 29.50; 53.70; 83.70$  nm<sup>-1</sup>  
46 (Fig. 1) after heat treatment at  $T_s=380$  K are crystallized in the structure of chalcopyrite  
47 tetragonal lattice  $\text{CuGaS}_2$  with periods  $a=0.535; c=1.047$  nm, CBC  $I\bar{4}2d$  [5].

## 48 2. Experiment

49 Parameters of  
50 short range order distances of coordination spheres and interatomic distances, coordinatio

51 numbers (CN) may be determined by the functions of atom radial distribution (FARD) pr  
 52 epared according to the retraining Fourier intensity of the coherent scattering of electrons.

$$53 \quad 4\pi r^2 \sum_m K_m \rho_m(r) = 4\pi r^2 U_0 \sum_m K_m \frac{2r}{\pi} \sum_m K_m \int_0^\infty St(s) \sin(Sr) dS \quad (1)[12],$$

54 Here  $U_0 = d/Mm_H$  - average density of atoms,  $d$  - amorph object density,  $M$  - molecular  
 55 mass,  $m_H = 1.65 \times 10^{-24}$  gr - hydrogen atom mass  $\rho_m(r)$  - function of atom density.  $S =$   
 56  $4\pi \sin \theta / \lambda$  is the half of scattering angle,  $K_m^2 = (Z_m / Z_1)$  (8) - scattering capability of  
 57 atoms and  $Z_m$  - the order number of the atom included in the content of expression,  $Z_1$  -  
 58 the order number of lighter atom of the expression in the periodical system.

$$59 \quad I(S) = \left( \frac{I_h(S)}{\sum_m I_m^2(S)} - 1 \right) \sum_m K_m \quad (9) \quad - \quad \text{interferention} \quad \text{function} \quad .$$

60 Reliable, (FARD) can only be obtained when integrating from 0 to  $\infty$  or before  $S_2$ ,  
 61 if interference functions do not feel out of oscillate that occurs in strongly disordered  
 62 systems. The intensity of scattering can be determined experimentally with sufficient  
 63 accuracy only on some interval of values  $S = 4\pi \sin \theta / \lambda$ , so practically the integration in  
 64 (1) is over a finite interval from  $S_1$  to  $S_2$ .

65

### 66 3. Results and discussion

67 Intensity curve electron scattering from amorphous films  $\text{CuGaS}_2$  were obtained on electr  
 68 onography brand EMR-102 in the form of graphs of dependences  
 69 of the intensity of scattering angles, i.e. from  $S = 4\pi \sin \theta / \lambda$  (Fig.1).

70 Function  $i(S)$

71 graphically depicted in (Fig 2.), were used to calculate (FARD) for  $\text{CuGaS}_2$  (Fig. 3.) accor  
 72 ding to formula (1). The calculation was carried out on the programmer "RADIADIS" on

73 the computer IBM. Intervals of variables accounted for  $\Delta r = 0,01 \text{ nm}^{-1}$ ,  $\Delta S = 0,01 \text{ nm}^{-1}$ .  
74

75 (FARD)  $\text{CuGaS}_2$  (Fig. 3.) contains four asymmetric highs one of which is isolated and a  
76 group of false highs, emanating from the larger values of S.

77 The area under the respective highs, manifesting themselves in  $r_1 = 0,234$ ;  $r_2 = 0,244$ ;  
78  $r_3 = 0,282$ ;  $r_4 = 0,411 \text{ nm}$ . are equal  $\Delta_1 = 16,0$ ;  $\Delta_2 = 20,3$ ;  $\Delta_3 = 55,5$  and  $\Delta_4 = 80,0$   
79  $\text{nm}$  respectively.

80 Distance  $r_1 = 0,234 \text{ nm}$  revealed on (FARD)  $\text{CuGaS}_2$ , is the distance between  
81 atoms Cu-S, as tetrahedral covalent radii are equal to  $r_{\text{Cu}} = 0,135$  and  $r_{\text{S}} = 0,104$   
82  $\text{nm}$ . Appropriate coordination number  $n = 4,1$  obtained from calculating the area  
83 under the first peak, also indicates tetrahedral surrounded by atoms of copper  
84 and gallium.

85 Radius of the second coordination sphere equal to  $r_2 = 0,244 \text{ nm}$  which could be  
86 able to interpret as the distance Ga-S. The ionic radii of gallium and sulfur atoms  
87 constitute  $r_{\text{Ga}} = 0,127$  and  $r_{\text{S}} = 0,104 \text{ nm}$ , for which coordination number is six.

88 Meaning coordination number equal to  $n_2 = 6,3$  received by us from calculating  
89 the area of the second peak on (FARD)  $\text{CuGaS}_2$  also indicates the octahedral environment  
90 of gallium atoms by sulfur atoms.

91 The bond length between the atoms equal to  $r_3 = 0,282 \text{ nm}$  corresponds to the  
92 distance between the same atoms Ga-Ga. Fourth maximum detected at a distance  
93  $\text{nm}$  can be referred to the distance between the negatively charged divalent atoms ( $\text{S}^{2-}$ ).

94 It should be noted that on (FARD)  $\text{CuGaS}_2$  arise false details too, and they  
 95 may arise due to errors in the experimental intensity curve or cliff: they are mainly manifes  
 96 ted in the large values of  $S$  and belong to groups with slightly blurred large  
 97 coordination number equal to 8, 10 and 12.

98 During the deposition of this ternary compound on the substrate with  $T_s = 423$ -  
 99  $433$  K a mixture of polycrystalline with single crystal is formed (Fig. 4.).

100 On the electronograms from the shown mixture appear more additional weaker  
 101 reflexes. As a result of increase in temperature  
 102 intensity polycrystalline lines are reduced but the intensity of  
 103 point reflections corresponding to single crystal grow.

104 Further increase of the substrate temperature to  $453$  K LiF leads to the formation of  
 105 a perfect single crystal. On electron diffraction from single crystals  
 106 (Fig. 5), discontinued at right angles strong point reflexes, forming a square grid  
 107 displayed on the basis of  $hk0$  reflexes known lattice  $\text{CuGaS}_2$ . Indexing of all  
 108 reflexes, including additional low intensity lines is achieved with parameter  
 109  $a = 1.605$  nm.

110 Period "c", established by electron diffraction, shot at an angle  $\varphi = 35^\circ$  was found to be  
 111  $2.102$  nm.

112 Between periods of lattices of the initial phase and superstructure there  
 113 are simple relations common with:  $a \approx 3a_0$ ;  $c \approx 2c_0$ . In the electron derived from film  
 114 on substrates formulated with higher temperatures ( $T_s = 473$  K), dynamic effects  
 115 appear (Fig. 6). The microstructure of single-

116 crystal layers  $\text{CuGaS}_2$  from which there is a dynamic high energy electron scattering is sho  
 117 wn in Fig. 7 (X 20000). Thus, substrates can be LiF  $\text{CuGaS}_2$  samples with varying substruc

118 ture including a super lattice phase super period. Growth mechanism of single-crystal  
119 thin - film and nano scale epitaxial films is a model for many heterogeneous and  
120 topochemical processes.

121 However, the existing theory of crystallization cannot explain all of the results of a large a  
122 mount of experimental work -

123 there is a clear discrepancy between the flow :The totality of new facts and their level of th  
124 eoretical understanding of the experimentally observed facts with a unified position cannot  
125 be considered. In existing theories of crystallization there is still no consensus on  
126 what is the main factor in orienting epitaxial.

127 Generally accepted explanation is not considered as such a statement and that the main fact  
128 or in orienting epitaxial is a single-crystal structure -

129 substrates. Focused on the growth of amorphous boundary layers prepared on the surface o  
130 f the substrate crystals [6,7], is proof that the basic structure of crystals does not  
131 determine substrate orientation effects .

132 Oriented crystallization on the outside boundary of polycrystalline layers [8-  
133 9], as well as the growth of not only epitaxial films, but also highly perfect single  
134 crystals through the amorphous boundary  
135 layers [10] makes relate to the theory of crystallization based on the structure of single-  
136 crystal substrates seeds very carefully. Since many experimental  
137 works performed revealed a clear discrepancy between the facts and their level of theoretic  
138 al understanding, it is not yet possible to formulate some general criteria for the formation o  
139 f epitaxial films and single crystal. Therefore, conditions for the formation of single-  
140 crystal films to day, as shown in the previous chapter, are  
141 established only experimentally.

142 Since the bulk crystal lattice  $\text{CuGaS}_2$  is ordered, in order to explain the  
 143 formation of super lattice phase we  
 144 should assume that it is the disordered phase. Disordering ordered - structures  
 145 some of the initial  
 146 of the atoms in it are defective, resulting superstructure should have a statistical average fr  
 147 equency. Regularities of similar phase transitions were first established for the phases of  
 148 the chemical group of compounds  $\text{A}^3\text{B}^3\text{C}_2^6$  [4].  
 149 Superstructure phase  $\text{CuGaS}_2$  is  
 150 oriented (100) plane parallel to the faces [11] LiF. During epitaxial growth on LiF  $\text{CuGaS}_2$   
 151 one unit cell (UC) superstructure is  
 152 mated with four cells of the substrate. Relative discrepancy mating crystal lattices in this  
 153 case is 2,9%.

#### 154 4. Conclusions.

155 In  $\text{CuGaS}_2$  amorph layers short range order parameters have been studied and it is  
 156 shown that distance  $r_1 = 0,234$  nm revealed on (FARD)  $\text{CuGaS}_2$ , is the distance  
 157 between atoms Cu-S, as tetrahedral covalent radii are equal to  $r_{\text{Cu}} = 0,135$  and  
 158  $r_{\text{S}} = 0,104$  nm. Appropriate coordination number  $n = 4,1$  obtained  
 159 from calculating the area under the first peak, also indicates  
 160 tetrahedral surrounded by atoms of copper  
 161 and gallium. Radius of the second coordination sphere equal to  $r_2 = 0,244$  nm which  
 162 could be able to interpret as the distance Ga-S. The ionic radii of gallium and  
 163 sulfur atoms constitute  $r_{\text{Ga}} = 0,127$  and  $r_{\text{S}} = 0,104$  nm, for which

164 coordination number is six. Meaning coordination number equal to  $n_2 = 6,3$   
 165 received by us from calculating the area of the second peak on (FARD) CuGaS<sub>2</sub> also i  
 166 ndicates the octahedral environment of gallium atoms by sulfur atoms. It is  
 167 shown that thin films on different substrates crystalize after thermal processing.  
 168 During the deposition of this ternary compound on the substrate with  $T_s = 423-$   
 169  $433$  K a mixture of polycrystalline with single crystal is  
 170 formed. Further increase of the substrate temperature to  $453$  K LiF leads to the  
 171 formation of a perfect single crystal.  
 172 Superstructure phase CuGaS<sub>2</sub> is oriented (100) plane parallel to the faces [11] LiF.  
 173 During epitaxial growth on LiF CuGaS<sub>2</sub> one unit cell (UC) superstructure is  
 174 mated with four cells of the substrate. Relative discrepancy mating crystal lattices in  
 175 this case is 2,9%.  
 176 It is found that between periods of lattices of the initial phase and superstructure  
 177 there are simple relations common with:  $a \approx 3a_0$ ;  $c \approx 2c_0$ .

178

179 **Literature**

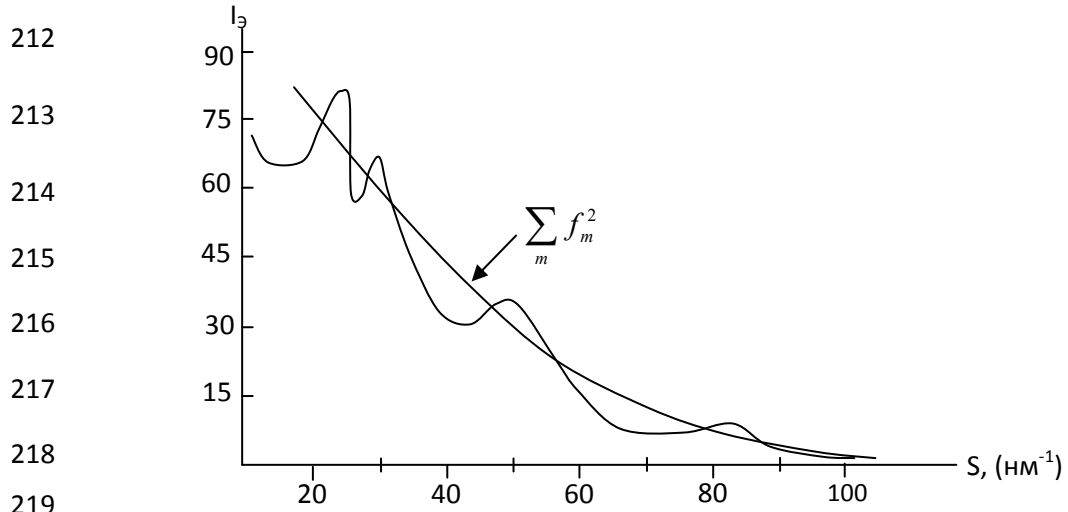
- 180 1. Bodnar I.V., Rud V.Y., Rud J.V., Breeding and research properties of ternary compounds  
 181 CuGa<sub>3</sub>Se<sub>5</sub> // Neogame. 2002, I. 38, № 9, p-875.
- 182 2. Bodnar I.V., Rud and V.Y., Rud Y.V. Novel I-III-VI<sub>2</sub> semiconductor-native protein structures  
 183 and their photosensitivities // Semicond. Science and Technology. 2002, v. 17, N 10, pp. 1044-  
 184 1047.
- 185 3. Orlova N.S., Bodnar I.V., Kushner T.L., Kudritskaya E.A. Crystal Growth and properties of  
 186 the Compounds CuGa<sub>3</sub>Se<sub>5</sub> and CuIn<sub>3</sub>Se<sub>5</sub> // Cryst. Res. Techn. 2002. v. 3, N 6, pp. 540-550.

- 187 4. Ismailov D.I. Phase formation, structure and kinetics crystallization in thin films  $A^3-B^3-C_2^6$ ,  
188 epitaxial growth superstructural phases. Dis.... d.f-m.n. Baku, 2007, P 345 .
- 189 5. Foseco-chemical properties of semiconductor materials : / Handbook Ed. Novoselova AVI  
190 Lazareva V.B. Moscow, Nauka, 1979, P 349
- 191 6. B.K. Vainshtein Structural electronography. M: Izd. An SSSR, 1956, P 315 .
- 192 7. Gerasimov, Y.M. of Distler GI Orientirovannayakristallizatsiya gold on the surface of the  
193 crystal NaU through amorphous carbon film // Kristallografiya, 1969, I. 14, number 6, pp. 1101-  
194 1104.
- 195 8. The distler GI Tokmakova E.I. Issledovanie epitaxial Rasta sulfur lead through boundary  
196 amorfnykh copying the electrical structure of the surface of crystals // crystallography, 1971, T.  
197 16, no 1, pp. 212-217.
- 198 9. The distler GI of Obrosof V.G. Photoelectron mechanism dalnodeystvie transmission and  
199 storage of structural information polikristallicheskom and single crystal boundary layers // Dokl.  
200 An SSSR, 1971, so 197, № 4, pp. 819-832.
- 201 10. Discharge Lobachev A.N. V.P. Vlasov other new method of breeding single crystals // Dokl.  
202 An SSSR, 1974, so 215, № 1, pp. 91-94.
- 203 11. Bodnar I.V., Bodnar IT, Viktorov I.A., O. Obratsova. Cultivation, structure and optical  
204 properties of single crystals triple connection  $CuGa_5Se_8$ // ZhPS, 2005, so 62, no. 1, pp. 544-548.
- 205 12. Nureyev M.A. Phase formation and phase transitions in thin films of the ternary system Cu-  
206 In- Se. Dis .....c.f-m.n Baku 1986. P 124 .
- 207
- 208

209

210 **Figures of ELECTRON DIFFRACTION AND ELECTRON MICROSCOPY STUDY OF FILMS CuGaS<sub>2</sub>.**

211



219

220 Fig. 1.

221

222

223

224

225

226

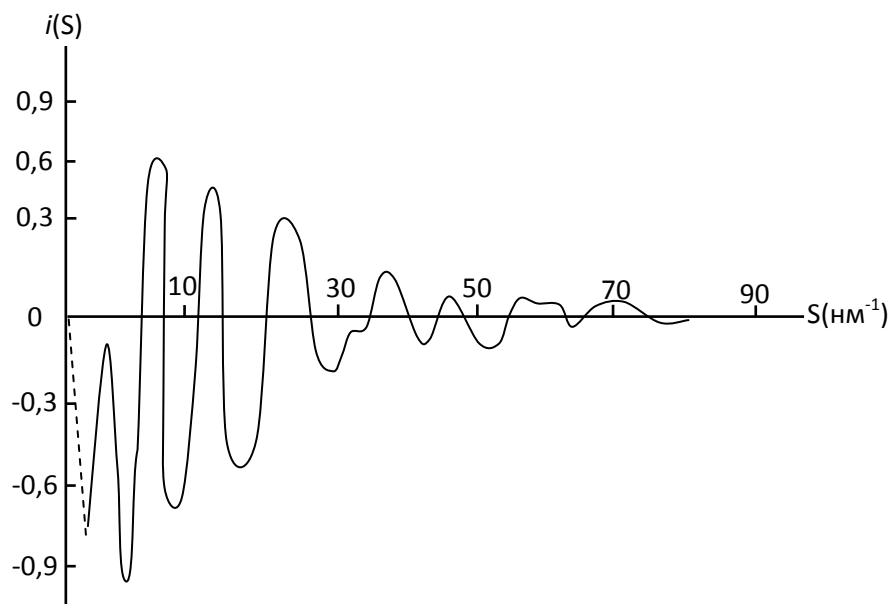
227

228

229

230

231



232

233

Fig.2.

234

235

236

237

238

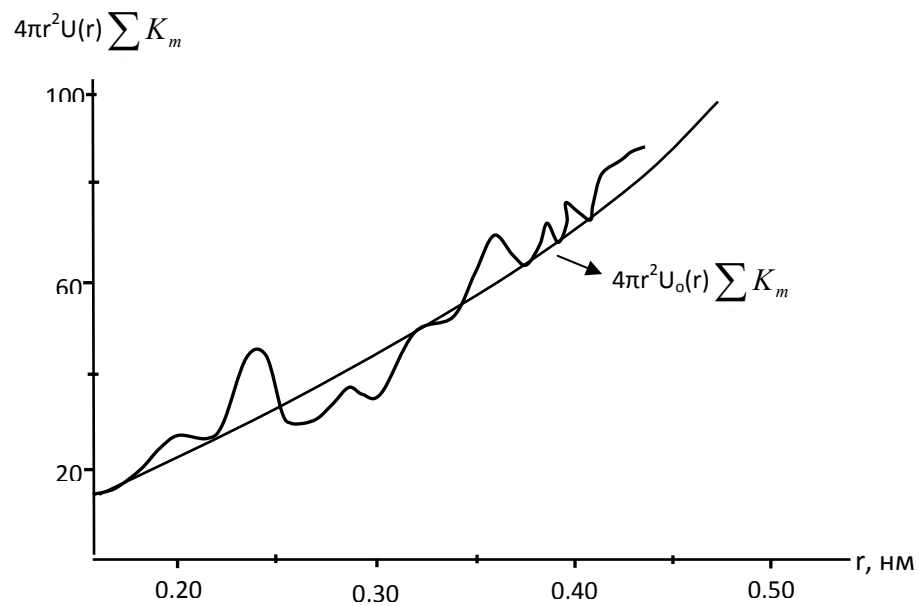
239

240

241

242

243



244

245

246

247

248

249

250

251

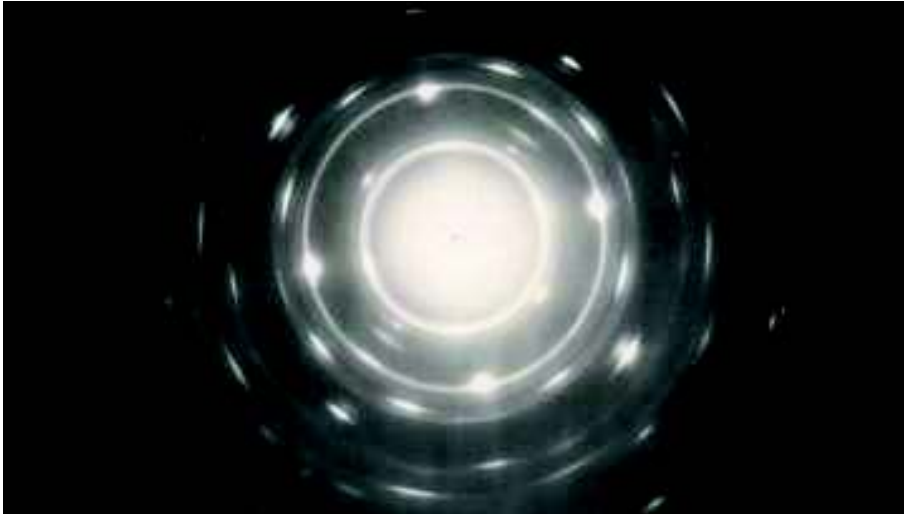
252

253

254 Fig. 3.

255

256



257

258

259 Fig. 4.

260

261

262

263

264

265

266

267

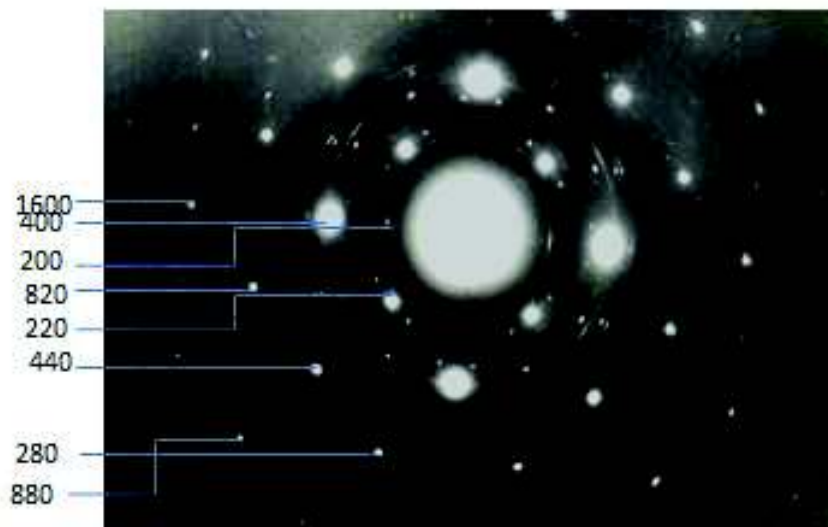
268

269

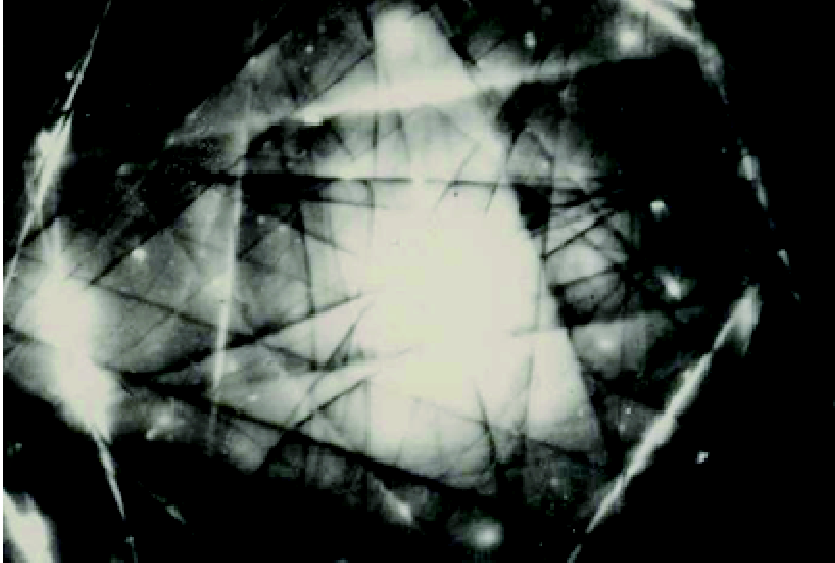
270

271

272

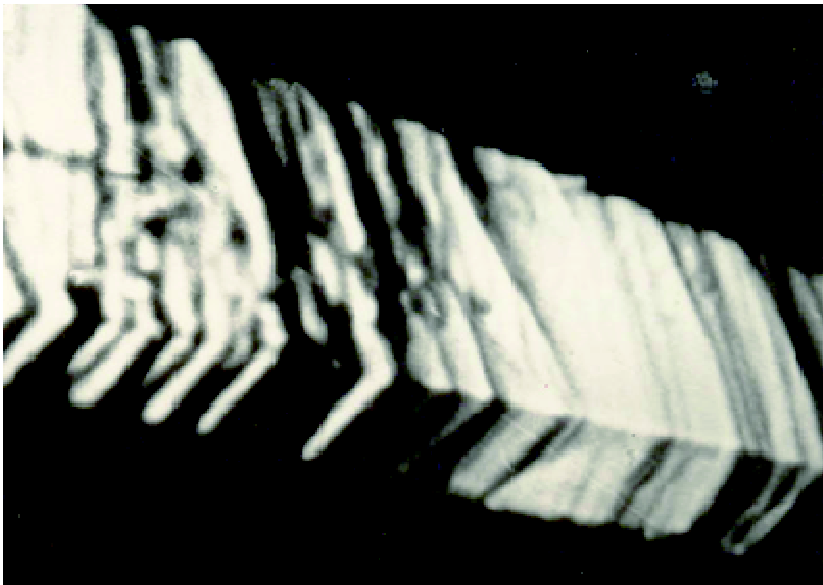


273  
274 Fig.5  
275  
276  
277  
278  
279  
280  
281  
282



283  
284  
285  
286

Fig.6.



287  
288

Fig. 7.

289	
290	
291	
292	Captions to figures of <b>ELECTRON DIFFRACTION AND ELECTRON</b>
293	<b>MICROSCOPY STUDY OF FILMS CuGaS<sub>2</sub>.</b>
294	
295	Fig.1. The intensity curves of amorphous CuGaS <sub>2</sub> .
296	
297	Fig.2. Interference scattering function of electrons of amorphous CuGaS <sub>2</sub>
298	
299	Fig.3. The curve of radial distribution of atoms of CuGaS <sub>2</sub>
300	
301	Fig. 4. Electron diffraction single crystal mixture with polycrystalline CuGaS <sub>2</sub>
302	
303	Fig.5. Electron diffraction from single crystal super lattice phase CuGaS <sub>2</sub>
304	
305	Fig.6. Electron diffraction pattern with Kikuchi lines from
306	
307	single crystal CuGaS <sub>2</sub> high perfection.
308	
309	Fig. 7. The microstructure of single-crystal beds of CuGaS <sub>2</sub> (H20000) .
310	